NUC TP 251

SPRAY DRAG OF SURFACE-PIERCING STRUTS

by
Richard B. Chapman
Sensor And Fire Control Department

September 1971

38

UNCLASSIFIED

Security Classification

DOCUMENT CONTROL DATA - R & D

(Security classification of title, body of abstract and indexing annotation must be entered when the overall report is classified)

1. ORIGINATING ACTIVITY (Corporate author)	2a. REPORT SECURITY CLASSIFICATION
Naval Undersea Research and Development Center San Diego, California 92132	UNCLASSIFIED 2b. GROUP

3. REPORT TITLE

SPRAY DRAG OF SURFACE-PIERCING STRUTS

4. DESCRIPTIVE NOTES (Type of report and inclusive dates)

Research and Development

5. AUTHOR(S) (First name, middle initial, last name)

Richard B. Chapman

6. REPORT DATE	7a. TOTAL NO. OF PAGES	7b. NO. OF REFS
September 1971	40	7

8a. CONTRACT OR GRANT NO.	9a. ORIGINATOR'S REPORT NUMBER(S)
Sponsored by the NUC Independent Exploratory and Development Funds as part of the "New Vehicle and Sonar Studies." b. PROJECT NO. c. d.	TP 251 9b. OTHER REPORT NO(S) (Any other numbers that may be assigned this report)

10. DISTRIBUTION STATEMENT

Distribution of this document is unlimited.

11. SUPPLEMENTARY NOTES	12. SPONSORING MILITARY ACTIVITY
	Naval Material Command Washington, D. C. 20360

13. ABSTRACT

Spray drags were measured using a series of nine surface-piercing struts operated in fourteen configurations. Empirical equations were deduced and compared with earlier data. The strut surface-area wetted above the waterline by the spray sheet was determined from photographs of various configurations and used as evidence that the frictional drag of the spray sheet flowing over the strut was the primary source of the measured spray drag. The mass flow rate contained in the spray sheet was measured indirectly. Following these experiments horizontal spray rails were attached to three of the struts and produced significant reductions in the spray drag of each.

Details of illustrations in this document may be better studied on microfiche

DD FORM 1 NOV 65 1473 (PAGE 1)

0102-014-6600

UNCLASSIFIED

Security Classification

14. KEY WORDS	LINK A		LINK B		LINK C	
	ROLE	WT	ROLE	WT	ROLE	WT
Naval architecture						
Hydrodynamic configurations						
Hydrofoil						
Drag						

NAVAL UNDERSEA RESEARCH AND DEVELOPMENT CENTER, SAN DIEGO, CA. 92132

AN ACTIVITY OF THE NAVAL MATERIAL COMMAND

CHARLES B. BISHOP, Capt., USN
Commander

Wm. B. McLEAN, Ph.D.
Technical Director

The work reported was done from September to November 1970, and was sponsored by the NUC Independent Exploratory and Development Funds as part of the "New Vehicle and Sonar Studies."

Released by
T. G. LANG, Head
Advanced Concepts Group

Under authority of
W. D. SQUIRE, Head
Sensor and Fire
Control Department

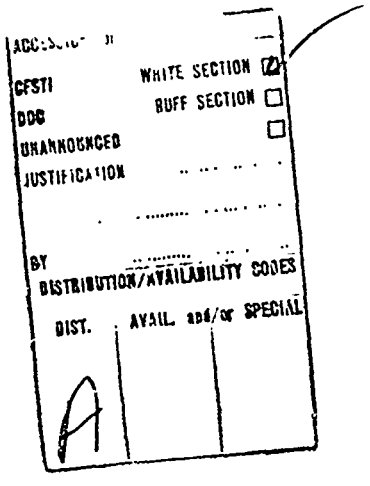

SUMMARY

PROBLEM

Determine the amount of spray drag acting on surface-piercing struts suitable for use on a semi-submerged ship and investigate ways of reducing spray drag.

RESULTS

Tests using a series of nine strut models in fourteen configurations resulted in empirical equations for spray drag. Photographs furnished evidence that spray drag is primarily due to the increased wetted surface area caused by the flow of the spray sheet over the strut surface above the waterline. Struts with blunt leading edges, such as airfoils, caused the spray to climb the strut at a steep angle. The mass flow rate contained in the spray sheet was measured indirectly to illustrate the high drag which could result from the spray striking trailing components of the ship. Horizontal spray rails were found to reduce spray drag significantly.

RECOMMENDATIONS

Symmetric double-arc struts with thickness to chord ratios of 16 percent or smaller are recommended for semi-submerged ships. Horizontal spray rails are recommended as a means of reducing spray drag.

CONTENTS

INTRODUCTION

Work was done to determine the amount of spray drag acting on a surface-piercing strut suitable for use on a semi-submerged ship. Means of reducing this drag were also investigated. A semi-submerged ship concept has been recently developed at NUC (reference 1). The ship consists of a pair of totally submerged hulls connected to a platform held above the waterline by two pairs of surface-piercing struts. The struts are designed to operate in the supercritical Froude number range to eliminate wave drag. Wave drag reaches a maximum when the Froude number based on chord length is approximately .5 (reference 2). Wave formation and wave drag drops off rapidly at higher Froude numbers and is replaced by a thin film of water which flows over the strut above the waterline leaving a spray sheet behind the trailing edge. Data presented in references 2 and 3 indicate that wave drag is negligible and spray drag is independent of Froude number for Froude numbers of about three or greater. Spray drag can be important at high Froude numbers, and a means of reducing such drag is desirable in designing struts for the semi-submerged ship.

A limited amount of previous data on spray drag is available. Hoerner (reference 2) combined his own results with data from Coffee and McKann (reference 4), Kaplan (reference 5), and others to deduce the empirical relationship

$$D_{spray} = 0.24qt^2 \tag{1}$$

for thickness to forebody ratios (x/c) less than about 0.4, and

$$D_{spray} = 0.12qt^2 \tag{2}$$

for blunter bodies. Savitsky and Breslin (reference 3) measured the spray drags for a series of airfoils with t/c = 10, 20, and 30% and x/c = 30%. From their data they deduced

$$D_{spray} = 0.03\,qct + 0.08qt^2 \tag{3}$$

Equation (3) results from fitting a straight line for D_{spray}/qct over a limited range of t/c and does not contain the discontinuity apparent in equations (1) and (2). The spray drags measured by Savitsky and Breslin are clearly greater than those predicted by Hoerner, perhaps because they used relatively blunt airfoils. This difference suggested that strut form may be an important factor in spray drag. To gain further insight into the problem of spray drag for various strut forms, measurements were made using a series of strut models.

DESCRIPTION OF THE STRUT MODELS

Nine strut models were fabricated from wood. Five of these were also tested with the direction of flow reversed, making a total of fourteen configurations. The first eight models had no angle of rake and six-inch chords. The ninth was raked 45° and had a chord length of $6\sqrt{2} \doteq 8.5$ inches. The first eight struts all had t/c ratios of 12, 16, or 21%. For each of these three ratios, two struts of the double arc type composed of two pairs of circular arcs were built, a symmetric strut with x/c = 50%, and an asymmetric strut with x/c = 35% or 65% depending on the direction of flow. The other three struts were a 16%-thick strut with a cusp on one edge and a wedge on the other, a 16%-thick 66-series airfoil, and a 16%-thick symmetric double-arc strut raked 45° to produce an effective t/c of about 11.3%. All struts had rounded tips and 0.25-inch wide sandstrips starting 0.75 inches from both leading and trailing edges. The nonraked struts were all 22-inches long. The strut forms are listed in table 1.

MEASUREMENT OF SPRAY DRAG

The strut models were tested in the Free Surface Water Tunnel at the California Institute of Technology with free-stream velocities of 20, 22, and 24 ft/sec. Based on a 6-inch chord these velocities correspond to Froude numbers between 5.0 and 6.0 and Reynolds numbers of about 10^6. These Froude numbers are sufficiently high to assure that the test data is in the Froude-number-independent region. Since the design Froude number for the semi-submerged ship is only about 2.0, a small amount of wave drag and other Froude-number-dependent components may be present in the spray drag of the ship. Velocities near the maximum speed of the tunnel were needed, however, to assure complete turbulence behind the sand strips and to minimize the effect of balance sensitivity. The measured values of section drag on the models indicate that the flow was turbulent.

Each configuration was tested at fifteen or more depths of submergence from a minimum of 3.4 inches. The drag on each strut was found to be a linear function of the submerged depth. The slope was identified with the two-dimensional section drag and the intercept was identified with the sum of the changes in drag due to the strut tip and the free surface. In equation form the relationship is

$$D_{total} = Xd + D_{spray} + D_{tip}, \tag{4}$$

where X is the section drag in lbs/ft. The tip drag was estimated using an empirical equation for rounded tips given in reference 2,

$$D_{tip} \sim -.02qt^2. \tag{5}$$

The negative tip drag is apparently due to the three-dimensional nature of the flow near the tip. This tip drag correction is roughly of the same magnitude as the scatter in the spray drag data.

An empirical formula for tip drag is not as satisfying as an analysis which eliminates tip drag entirely. This is theoretically possible using the pitching moment data. Let P(Z) be the pitching moment measured at an elevation Z above the waterline. It may be shown that

$$\frac{dP}{dZ} = XZ - D_{spray} . \tag{6}$$

Although equation (6) is theoretically superior, attempts to apply it were unsuccessful for two reasons. First it was necessary to extrapolate over a much greater distance using equation (6) since measurements for small values of Z could not be made without causing the spray to strike the drag balance. In addition, calculation of the first derivative increased the scatter in the data.

SPRAY DRAG RESULTS

Results of calculations using equations (4) and (5) are listed in table 1. Two spray drag coefficients are presented, C_0, based on the area ct, and C_1, based on the waterplane area A, an important parameter for the semi-submerged ship. The coefficient C_0 is plotted against t/c in figure 1 for struts of the double arc form. Also shown are empirical equations and data from references 2 and 3. A dependence of spray drag on strut form is evident in the present data. Struts with x/c = 35% produced the most spray drag and struts with x/c = 65% produced the least. Spray drag data for each group of double arc struts resemble the airfoil data from reference 3 in form but are closer to the data of reference 2 in magnitude. Lines similar to equation (3) were fitted for each of the three groups of double arc struts resulting in the following empirical equations:

$$C_0 = .003 + .06\ t/c \qquad \text{when } x/c = 65\%, \tag{7}$$

$$C_0 = .011 + .08\ t/c \qquad \text{when } x/c = 50\%, \tag{8}$$

and

$$C_0 = .009 + .013\ t/c \qquad \text{when } x/c = 35\%. \tag{9}$$

These equations are quite rough because of data scatter and the uncertainty of the tip drag estimate. However, they provide engineering estimates over a limited range of t/c.

Both the cusp and the wedge leading edges of strut 2 produce less drag than strut 1. After the waterplane area is taken into account, however, this advantage becomes negligible. The double-arc strut swept 45° appears to offer a savings in spray drag contrary to the conclusion of reference 4, based on airfoils swept 30°, that the spray drag of a swept strut depends only on its waterplane form.

COMPARISON WITH PREVIOUS RESULTS

The empirical formula of reference 2 is partially based on the spray drags of a 13%-thick symmetric double arc tested by Benson and Land, and a 15%-thick asymmetric double arc with x/c = 40% tested by Kaplan (reference 5). These strut forms are described in reference 6. The 13%- and 15%-thick double-arc struts produced C_0 coefficients of .026 and .028 respectively. These values are very close to those predicted by equation 9 and within 20% of those predicted by equation 8 Kaplan found that the 15%-thick double arc was not sufficiently asymmetric to cause a detectable change in the spray or section drag when the direction of flow was reversed. Hoerner also uses measurements apparently made with 15%- and 30%-thick struts with x/c = 40%. The shapes of these struts were not indicated, but they were probably double arcs. The spray drags of these struts were also independent of the direction of flow. The corresponding value of C_0 for both thicknesses was .036. This is about 50% greater than predicted by equation (8) for the 15%-thick strut but very close to the predicted value for the 30%-thick strut. In general the spray drags in reference 1 are larger than predicted by equation (8) but are not inconsistent when experimental error is taken into account.

Figure 2 shows the spray drags reported by Coffee and McKann (reference 4) for 12%- and 21%-thick 66-series airfoils together with the spray drag measured in the present experiment using a 16%-thick airfoil of the same series. The much lower spray drag of the reversed airfoil 8B again illustrates the influence of strut form. A unique feature of the 66-series airfoil data is that C_0 decreases as t/c increases. In interpreting this result one should perhaps keep in mind the uncertainty introduced by tip drag and the fact that the struts used by Coffee and McKann had square tips. A straight line fitted through the points in figure 2 gives the approximate formula

$$C_0 = .036 - .03\ t/c. \qquad (10)$$

Note that the spray drag of the airfoil is similar to that of the asymmetric double arc strut of the same thickness in either orientation. This indicates that spray drag is not simply a function of x/c but depends on the overall shape.

APPEARANCE OF THE SPRAY SHEET

The spray sheets appeared quite different for the various strut configurations. Photographs were made of ten representative configurations. The spray sheets produced at 10 and 24 ft/sec are shown in figures 3 through 12. The spray patterns at 10 ft/sec should resemble those on the full-sized ship since the Froude numbers are nearly equal. As these photographs show, spray is a somewhat misleading term for the smooth, continuous sheet which breaks up only after leaving the trailing edge. Separation of the sheet from the strut was never observed. The sheet is thickest near the free surface and grows thinner further up the strut until it is terminated by a thick lip of slowly moving liquid believed to result from momentum loss caused by skin-friction. Near the top the sheet is very thin and the liquid may lose most of its horizontal velocity and move downward under the influence

of gravity to collect in a lip. This should be most evident at low Froude numbers. The lip is, in fact, more obvious at lower speeds.

Note the differences in the spray sheets formed by the various struts. The sheet formed by the airfoil, figure 11, climbs the leading edge to over half a chord above the waterline. Similar behavior is displayed by sheets formed on airfoils shown in reference 4. In contrast sheets formed on double arc struts leave the waterline at various angles. Steeper angles are associated with greater spray drags. Another variation is the cusped strut configuration 2A which forms its sheet a small distance behind the leading edge.

SPRAY DRAG AS A FUNCTION OF WETTED SURFACE AREA

It is evident that strut configurations which produce large spray sheets also have large spray drags. This observation is made quantitatively in figure 13 which plots the spray drag of the photographed configurations at 24 ft/sec against the strut surface area wetted by the spray. Also plotted is the theoretical drag for turbulent flow at 24 ft/sec over a flat plate with a six-inch chord and surface area equal to the area wetted by the spray. In addition to experimental scatter there are a number of mechanisms which could cause the spray drag to depart from this value.

1. The horizontal component of the sheet velocity will not always equal the free stream velocity.
2. Flow of the spray sheet may not be fully turbulent.
3. Another drag mechanism is associated with the upward momentum imparted to the spray sheet. The corresponding flow energy is dissipated when the spray strikes the free surface behind the strut.
4. Although there is no evidence of spray sheet separation, the spray sheet may contribute some pressure drag above the waterline.
5. At small distances below the waterline the flow will not be purely two-dimensional. The spray may have a favorable effect of relieving pressure drag near the free surface. This effect may contribute to the low values of spray drag measures on struts with x/c = 65%.

Despite all these possible mechanisms, the total area wetted by the spray sheet appears to be the controlling factor in the spray drag of all photographed struts with the possible exceptions of configurations 3B and 5B. Note that the small spray drag coefficient of the swept strut, 9, can be explained by the small wetted surface area. In fact, strut 9 has more spray drag *per wetted surface area* than most other configurations. Assume that an unswept strut of the same waterplane form produces a spray sheet similar to the swept strut. Then it can be determined from the photograph that an additional, roughly triangular section of strut surface would be covered by the spray sheet, increasing the wetted area by about 35%. This would explain the difference between the spray drag coefficients for the swept strut 9, and the unswept strut 4, which has a similar waterplane form. This advantage might not be present, however, for struts such as airfoils which cause the spray to climb the strut's leading edge.

Figure 13 includes data from reference 4 for the 12%- and 21%-thick airfoils at 51 ft/sec. Since these foils had no turbulence stimulators, their section drag coefficients indicate that the skin-friction was less than in the fully turbulent case. To compensate for this reduced skin-friction, the spray drags of these points in figure 13 have been multiplied by the ratio of the section drag coefficient of strut 5A to that of the 12%-thick airfoil of reference 4. These compensated drags appear in figure 13 only. The uncompensated coefficients in figure 2 are consistent with the spray drag of strut configuration 8A. This suggests that a decrease in skin-friction increases the surface area wetted by the spray and leaves the spray drag coefficient relatively unchanged.

SECTION DRAG RESULTS

Table 2 lists the section drag of each strut configuration. Also listed are the section drag coefficients C_2 and C_3, which are based on the areas cd and $d\sqrt{A}$ respectively. The latter coefficient is of special interest for the semi-submerged ship since A and d are design parameters. The drag coefficient for a flat plate of the same size as the strut models was computed under the assumption that the flow is laminar up to the sand strips located 1/8 of the chord length behind the leading edge and is fully turbulent behind the strips. According to reference 7 the laminar and turbulent skin-friction coefficients are

$$C_L = 2 \times 1.3 \times (Vc/8\mu)^{-1/2} = .0071 \tag{11}$$

and

$$C_T = 2 \times .074 \times (Vc/\mu)^{-1/5} = .0093. \tag{12}$$

An average weighted over the length of the plate yields

$$C_{2f} = .0090. \tag{13}$$

The section drag coefficients of the struts are greater, of course, due to supervelocity and separation. The roughness of the sand strips also adds to the drag. Figure 14 shows C_2/C_{2f} as a function of t/c for the double-arc struts. According to reference 1 supervelocity for streamlined forms with $x/c \sim 30\%$ may be accounted for by adding the factor 2 t/c as indicated in the figure. This factor should apply for x/c = 35% and 65%. Note the large separation drag for struts with x/c = 65%. Singing due to the shedding of vortex sheets was observed for strut 7B.

FLOW RATE OF THE SPRAY SHEET

Measurement of the properties of the spray sheet affords insight into the problem of spray drag. A simple experiment of this type was made by measuring the thrust caused by the spray striking a large flat plate mounted about one foot behind the trailing edge of a strut. The bottom of the plate was held approximately a quarter of an inch above the

waterline. Measurements for each strut model were made at velocities of 20 and 24 ft/sec. In all cases the plate was ahead of the point where the spray would attain its maximum height in the absence of the plate. Of course a portion of the sheet leaving the trailing edge at a low angle and close to the waterline might fall back into the stream before striking the plate, but this portion is of little interest.

Table 3 lists the thrust T on the plate caused by spray sheets formed by each strut configuration. This thrust should equal the momentum flux of the spray striking the plate. Comparison with spray drags measured on the same struts indicate that spray drag can make a significant reduction in the momentum of the spray sheet, particularly for the thinner struts, but enough momentum is left to create a large pressure drag on any object the spray may strike. Also listed is the mass rate of flow M calculated using the approximation that spray drag is entirely due to slowing the spray sheet below the free stream velocity V. Then, the mean velocity of the spray leaving the strut is

$$V' = TV/(T + D_{spray}) \tag{14}$$

and the mass rate of flow is

$$M = (T + D_{spray})/V. \tag{15}$$

The mass flow appeared to be concentrated in the lower portion of the spray sheet. The mass rate of flow of roughly the upper three-quarters of the sheet formed at 24 ft/sec by strut 2B was measured by capturing the stream in a bucket. About 1.5 lbs/sec entered the bucket, indicating that the lower quarter of the sheet contained about half of the mass flow.

The mass rate of flow is nearly independent of strut form despite the wide range of forebody lengths. A coefficient based on strut thickness,

$$C_M = M/\rho\, Vt^2, \tag{16}$$

is presented in table 3. This coefficient should be a function of t/c and the Froude number. As shown in figure 15, the data is well represented by

$$C_M = 3.7\, Ft/c = 3.7\, Vt/c\sqrt{gc}. \tag{17}$$

It should be emphasized that this empirical equation is based on a very limited range of data. It is reasonable, however, to expect C_M to increase with Froude number in the supercritical range. Then skin friction will have a proportionally greater influence on the flow of the spray sheet at lower Froude numbers.

It is possible to estimate the drag caused by the upward acceleration of the spray. If M is the mass rate of flow and $\bar{h}$ is the mean maximum height attained by the fluid elements of the spray, this contribution to the drag is

$$D_v = M\bar{h}/V'. \tag{18}$$

In all cases this drag is a small fraction of the measured spray drag. For example, $M = 3.4$ lbs/sec and $V' = 20$ ft/sec for strut 1 at 24 ft/sec. A generous estimate for $\bar{h}$ is simply half the maximum height of the spray. An $\bar{h}$ of five inches results in a drag of about 0.07 lbs.

REDUCTION OF SPRAY DRAG

Strut drag, a combination of spray drag and section drag, may be minimized by a proper choice of the strut form. Struts as thick as 21% can be eliminated, but for fixed waterplane area and depth of submergence, the symmetric double-arc struts with $t/c = 12\%$ and 16% are nearly equivalent. With the exception of the swept strut, no strut form tested offers a significant advantage over strut 1. Struts with $x/c = 65\%$ are of little practical value due to high section drag and other undesirable effects. However, the relationship between spray drag and the surface area wetted by the spray suggests that drag can be reduced without altering the basic strut form by adding a device designed to reduce the wetted surface area. Three types were tested: vertical separation strips, a spray plate, and horizontal spray rails. Only the spray rails were successful in reducing drag.

A brief test was made with a pair of 1/8-inch thick vertical strips located two inches ahead of the trailing edge of strut configuration 3A. The strips were able to separate the spray sheet from the strut as intended but did not reduce drag. This was probably because additional pressure drag was exerted on the strips and the surface area wetted by the spray was reduced by only slightly more than one third.

A large flat plate was attached to strut 1 parallel to the flow, creating a spray shield. This did not appear to reduce the total wetted surface area since the spray sheet covered the underside of the plate in a pattern very similar to the flow over the strut in the absence of the plate. No measurable change in drag was observed.

Then, a series of spray rails was added to strut 1. Each rail was a 1/8-inch-thick wood strip steamed to conform to the strut and faired at both ends. The rails were mounted parallel to the flow with their centerlines 3/4-inches apart. A single rail was sufficient to turn the spray as shown in figure 16. These rails produced a substantial reduction in spray drag. In figure 17 the drag at 20, 22, and 24 feet per second on strut 1, both with and without rails, is plotted against the elevation of the upper edge of the strut. At 24 ft/sec a maximum reduction of .35 lb of drag occurs when the lowest set of rails is about 5% of the chord above the waterline. At an elevation of 20% of the chord, the savings is about 25 lbs.

Later, 1/16-inch-thick plastic rails were glued on struts 3 and 8, which were then tested in configurations 3A and 8A. Results are shown in figure 18. Ventilation was more severe when these rails were submerged since they were not faired. These rails reduced drag but not as much as those on strut 1. The maximum savings in both cases was about .25 lb. It was not determined whether the smaller drag reduction was due to the thinner rails or was characteristic of the strut forms; it is possible that attachment of a spray rail to a relatively blunt strut form, such as strut configurations 3A or 8A, causes water to pile up near the front of the strut and then separate, causing a pressure drag. In any case it is evident that the net effect of spray rails is to reduce drag.

CONCLUSIONS

The results of this investigation of the spray drag produced by fourteen strut configurations are briefly summarized in this section.

1. Spray drag is partially dependent on strut form as well as strut thickness. Struts with blunt leading edges tend to produce more spray drag.

2. Empirical equations were deduced for several strut series in the region $.12 \leqslant t/c \leqslant .21$. For double arc struts they are

$$D_{spray} = .003\ qct + .06\ qt^2 \text{ when } x/c = 65\%,$$

$$D_{spray} = .011\ qct + .08\ qt^2 \text{ when } x/c = 50\%,$$

and $$D_{spray} = .009\ qct + .13\ qt^2 \text{ when } x/c = 35\%.$$

The equation for the 66-series airfoil is

$$D_{spray} = .036\ qct - .03\ qt^2.$$

3. A cusped leading edge decreases spray drag but does not produce an advantage for a fixed waterplane area. Sweeping a double arc strut decreases the spray drag for a given waterplane area by decreasing the surface area wetted by the spray.

4. Skin-friction due to the wetting of the strut surface by the spray sheet is the primary source of spray drag.

5. The mass rate of flow in the spray sheet depends on t/c and the Froude number but not on x/c. However, blunter bodies send the spray up at higher angles wetting more strut area. Blunt sections are, therefore, not recommended for semi-submerged ships.

6. The losses caused by the upward acceleration of the spray contributed only a small fraction of the total spray drag of slender struts at moderate Froude numbers.

7. The momentum in the spray sheet is sufficient to create a large pressure drag on any object it may strike.

8. Horizontal spray rails can produce a substantial reduction in spray drag.

Table 1. Spray Drag and Spray Drag Coefficients for Various Strut Configurations.

Strut Configuration	Speed, ft/sec	t/c	x/c	Type*	Spray Drag, lb	C_0	C_1
1	24	.16	.50	D.A.	.515	.023	.035
1	22				.43	.022	.033
1	20				.40	.024	.036
2A	24	.16	.50	CSP	.37	.017	.030
2A	22				.34	.018	.032
2A	20				.305	.018	.033
2A	20				.30	.018	.032
2B	24	.16	.50	WDG	.375	.017	.030
2B	22				.355	.018	.033
2B	22				.335	.017	.031
2B	20				.28	.017	.030
3A	24	.16	.35	D.A.	.71	.032	.048
3A	22				.585	.031	.046
3A	20				.48	.030	.044
3B	24	.16	.65	D.A.	.225	.010	.015
3B	22				.21	.011	.016
3B	20				.225	.013	.020
4	24	.12	.50	D.A.	.37	.022	.033
4	22				.315	.022	.033
4	20				.255	.021	.031
5A	24	.12	.35	D.A.	.385	.023	.034
5A	22				.365	.026	.038
5A	20				.285	.024	.036

*D. A. = Double Arc
CSP = Cusped Leading Edge
WDG = Wedge Leading Edge

Table 1. (Continued).

Strut Configuration	Speed, ft/sec	t/c	x/c	Type*	Spray Drag, lb	C_0	C_1
5B	24	.12	.65	D.A.	.16	.010	.014
5B	22				.165	.012	.017
5B	20				.12	.010	.015
6	24	.21	.50	D.A.	.87	.030	.044
6	22				.695	.028	.042
6	20				.59	.029	.043
7A	24	.21	.35	D.A.	1.05	.036	.053
7A	22				.855	.035	.052
7A	20				.795	.039	.058
7B	24	.21	.65	D.A.	.475	.016	.024
7B	22				.400	.016	.024
7B	20				.345	.017	.025
8A	24	.16	.50	FOIL	.70	.031	.046
8A	22				.60	.032	.047
8A	20				.50	.032	.048
8B	24	.16	.50	REV	.28	.013	.019
8B	22				.23	.012	.018
8B	20				.26	.017	.025
9	24	.16	.50	SWP	.485	.015	.023
9	22				.43	.016	.022
9	20				.36	.016	.023

*D.A. = Double Arc
FOIL = 66-Series Foil
REV = Reversed Foil
SWP = Swept Strut

Table 2. Section Drag and Section Drag Coefficients for Various Strut Configurations.

Strut Configuration	Speed ft/sec	Section Drag lb/ft	C_2	C_3	Strut Configuration	Speed ft/sec	Section Drag lb/ft	C_2	C_3
1	24	3.44	.0123	.037	5B	24	3.60	.0129	.046
1	22	2.95	.0126	.038	5B	22	3.00	.0128	.045
1	20	2.42	.0125	.038	5B	20	2.52	.0130	.046
2A	24	3.41	.0122	.041	6	24	4.47	.0160	.043
2A	22	2.86	.0122	.041	6	22	3.81	.0162	.043
2A	20	2.32	.0119	.040	6	20	3.08	.0159	.043
2A	20	2.33	.0120	.040					
2B	24	3.40	.0122	.041	7A	24	4.05	.0145	.038
2B	22	2.83	.0120	.040	7A	22	3.54	.0151	.040
2B	22	2.92	.0124	.042	7A	20	2.89	.0148	.040
2B	20	2.49	.0128	.043					
3A	24	3.40	.0122	.037	7B	24	6.14	.0220	.058
3A	22	2.94	.0125	.038	7B	22	5.13	.0218	.058
3A	20	2.53	.0128	.040	7B	20	4.35	.0224	.060
3B	24	4.87	.0174	.053	8A	24	3.50	.0125	.038
3B	22	4.07	.0173	.053	8A	22	2.96	.0126	.038
3B	20	3.30	.0170	.052	8A	20	2.42	.0125	.037
4	24	3.02	.0108	.038	8B	24	4.78	.0171	.052
4	22	2.59	.0110	.039	8B	22	4.06	.0173	.053
4	20	2.22	.0114	.040	8B	20	3.23	.0166	.051
5A	24	2.99	.0107	.037	9	24	3.82	.0097	.035
5A	22	2.46	.0105	.037	9	22	3.23	.0097	.035
5A	20	2.12	.0109	.038	9	20	2.70	.0098	.036

Table 3. Mass Flow Rate and Mass Flow Rate Coefficients for Various Strut Configurations.

Strut Configuration	V ft/sec	T lb	M lb/sec	C_M
1	24	1.98	3.35	.349
	20	1.15	2.49	.312
2A	24	2.03	3.22	.335
	20	1.09	2.24	.280
2B	24	2.01	3.20	.334
	20	1.06	2.16	.270
3A	24	1.93	3.54	.369
	20	1.10	2.54	.318
3B	24	2.30	3.39	.353
	20	1.34	2.53	.316
4	24	.77	1.53	.283
	20	.43	1.11	.247
5A	24	.82	1.62	.301
	20	.47	1.22	.272
5B	24	.80	1.29	.238
	20	.42	.87	.193
6	24	4.61	7.35	.444
	20	2.86	5.55	.403
7A	24	4.19	7.02	.424
	20	2.36	5.08	.369
7B	24	3.54	6.72	.407
	20	2.50	4.58	.333
8A	24	1.68	3.19	.332
	20	.93	2.30	.288
8B	24	2.10	3.30	.344
	20	1.25	2.44	.306

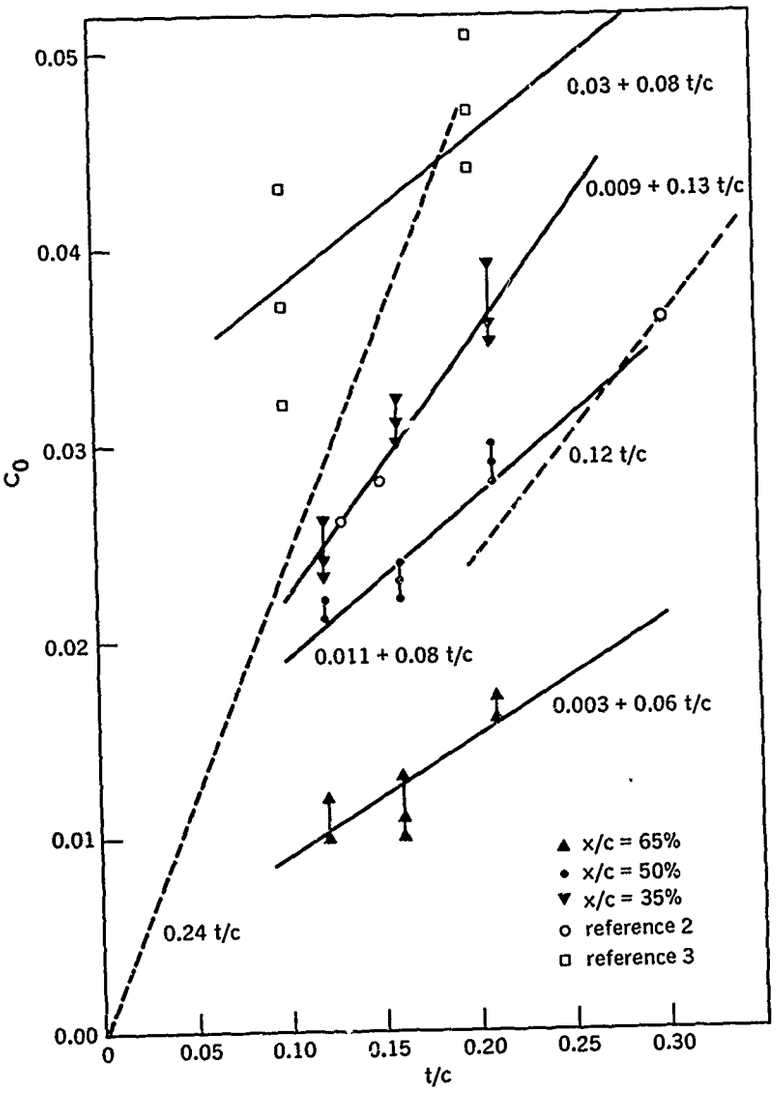

Figure 1. Spray drag coefficients for double arcs.

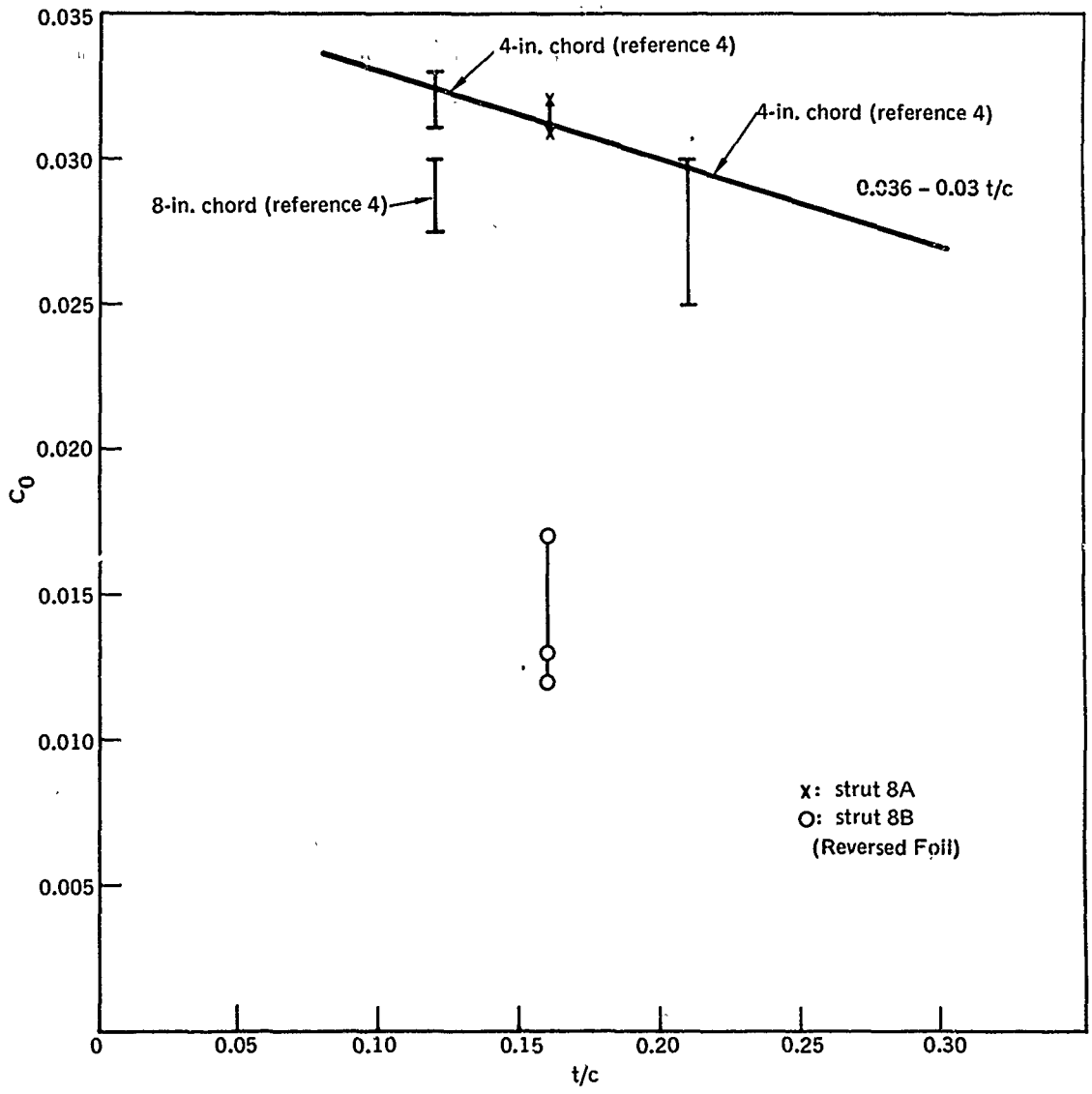

Figure 2. Spray drag coefficients for 66-series airfoils.

10 ft/sec

24 ft/sec

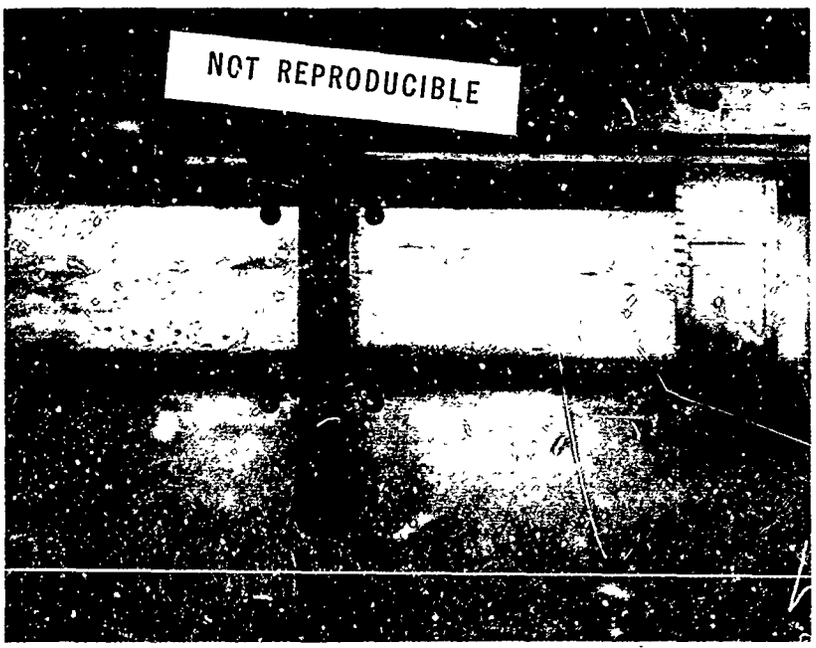

Figure 3. Spray sheets produced by strut 1 at 10 and 24 ft/sec where t/c = 0.16 and x/c = 0.50.

10 ft/sec

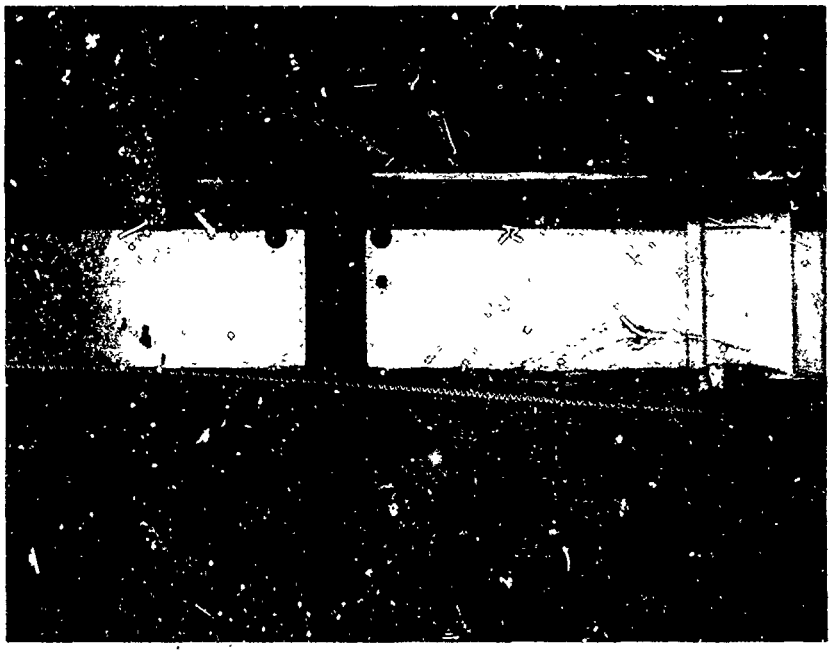

24 ft/sec

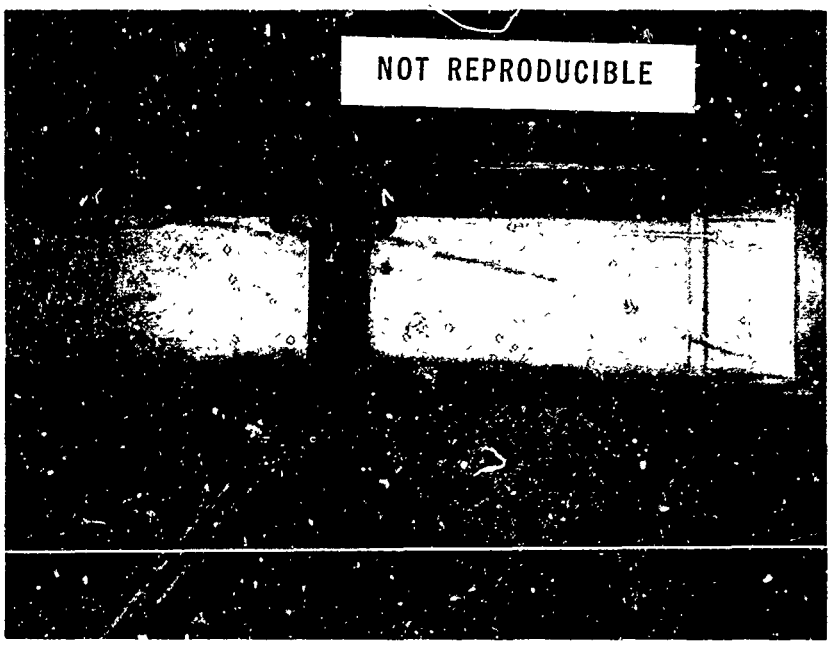

Figure 4. Spray sheets produced by strut 2A at 10 and 24 ft/sec where t/c = 0.16 and x/c = 0.50 (Cusped).

10 ft/sec

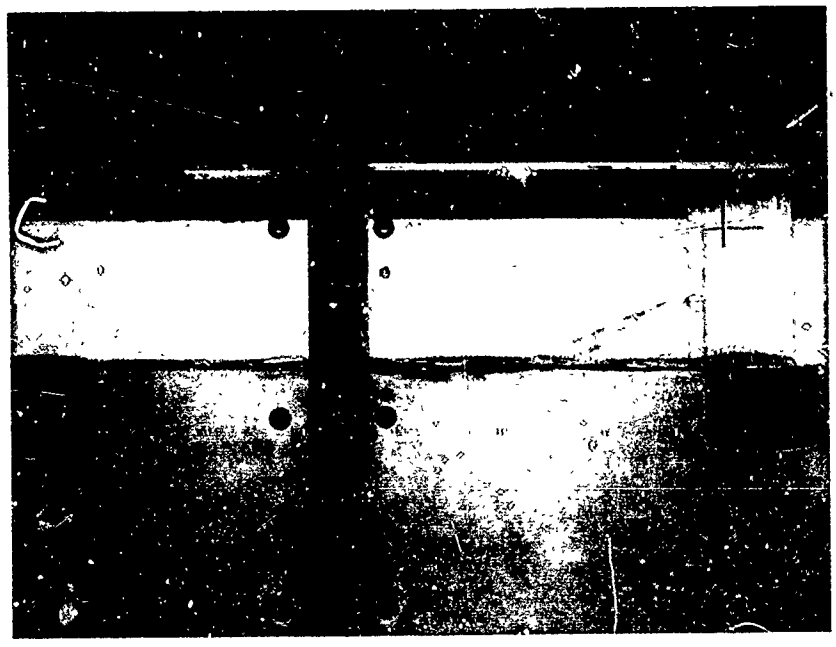

24 ft/sec

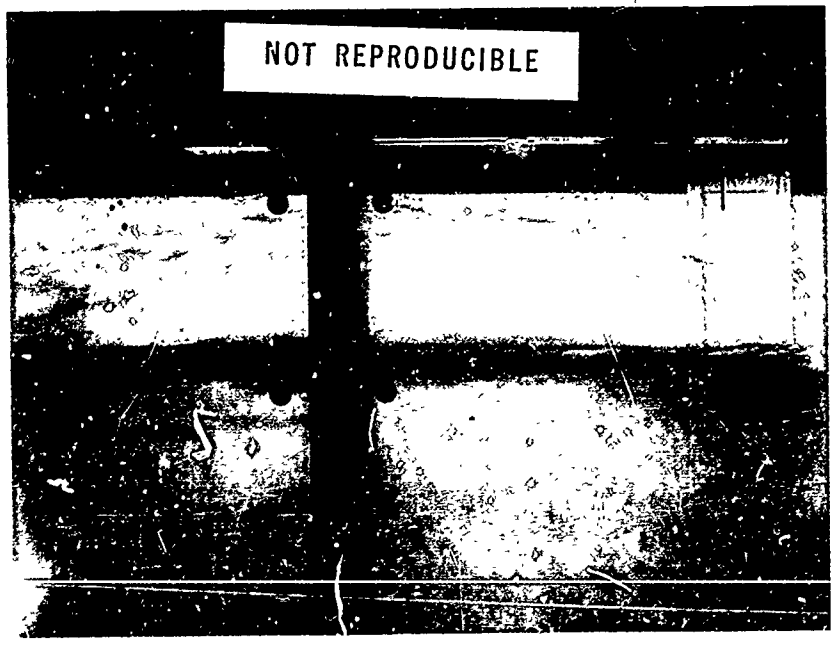

Figure 5. Spray sheets produced by strut 3A at 10 and 24 ft/sec where t/c = 0.16 and x/c = 0.35.

10 ft/sec

24 ft/sec

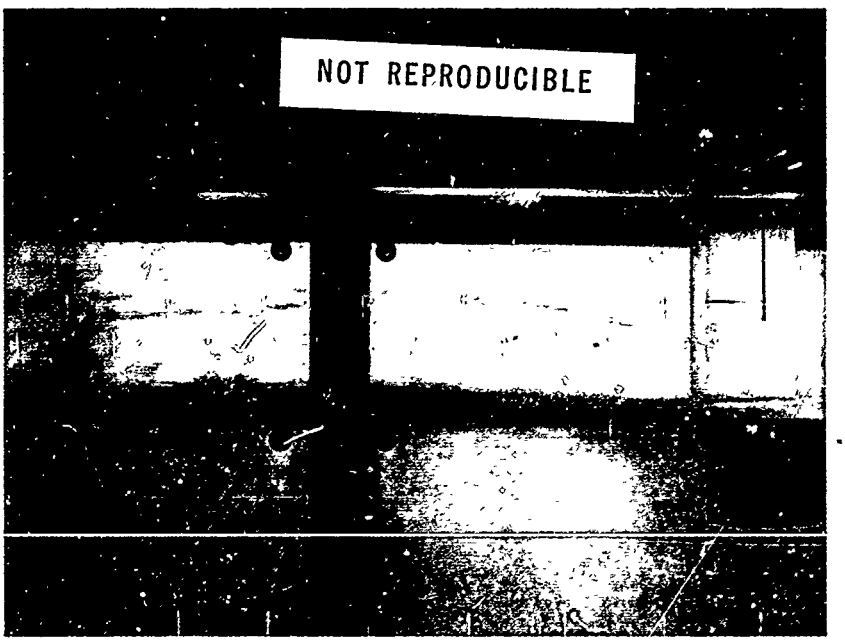

Figure 6. Spray sheets produced by strut 3B at 10 and 24 ft/sec where t/c = 0.16 and x/c = 0.65.

10 ft/sec

24 ft/sec

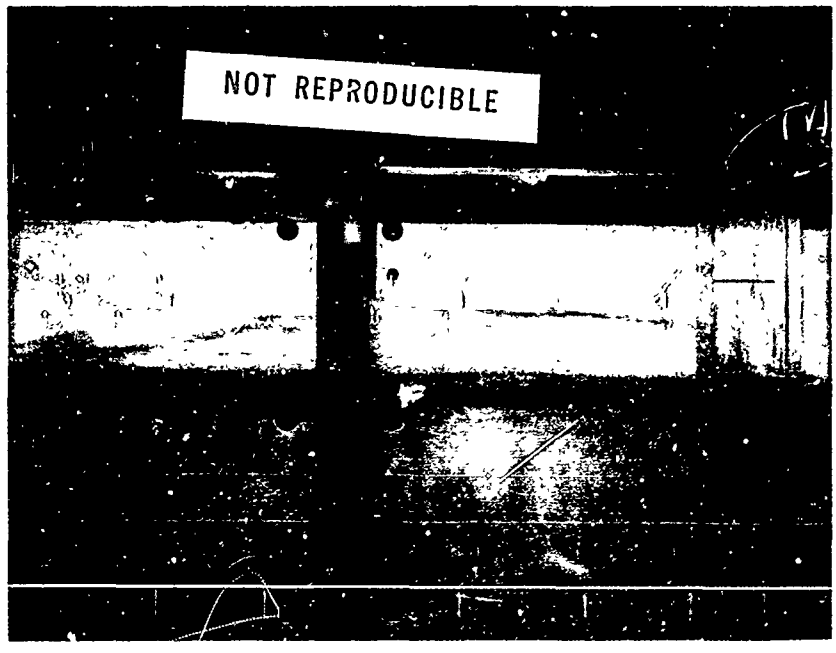

Figure 7. Spray sheets produced by strut 4 at 10 and 24 ft/sec where t/c = 0.12 and x/c = 0.50.

10 ft/sec

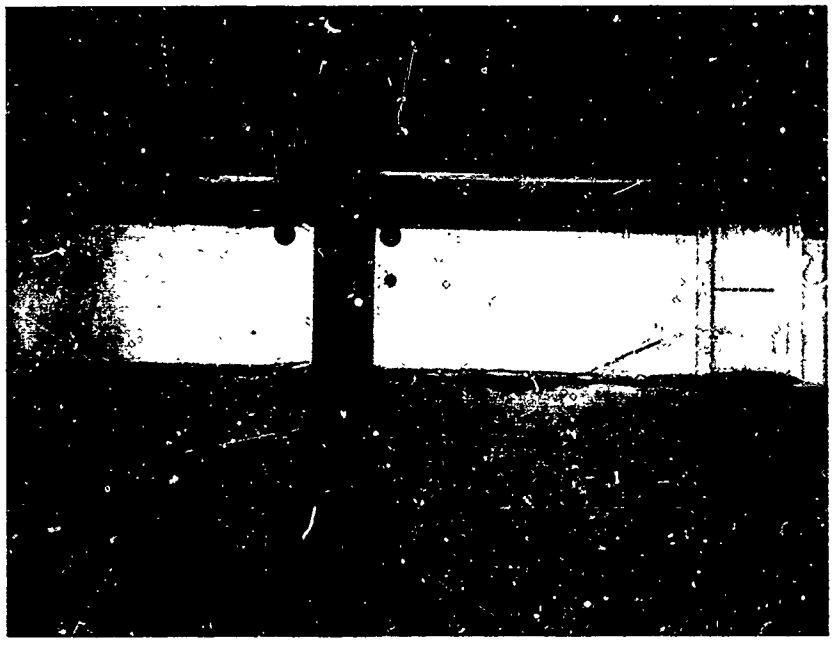

24 ft/sec

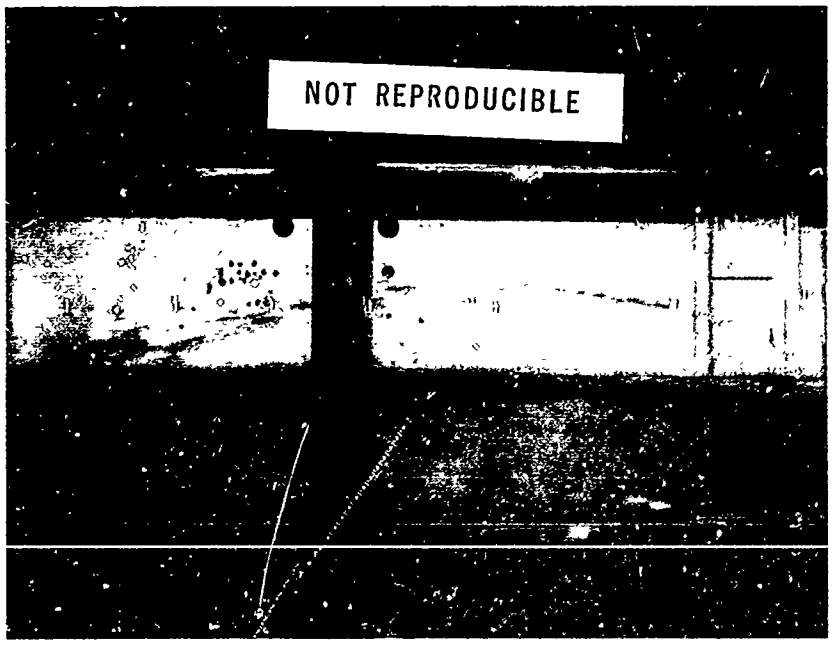

Figure 8. Spray sheets produced by strut 5A at 10 and 24 ft/sec where t/c = 0.12 and x/c = 0.35.

10 ft/sec

24 ft/sec

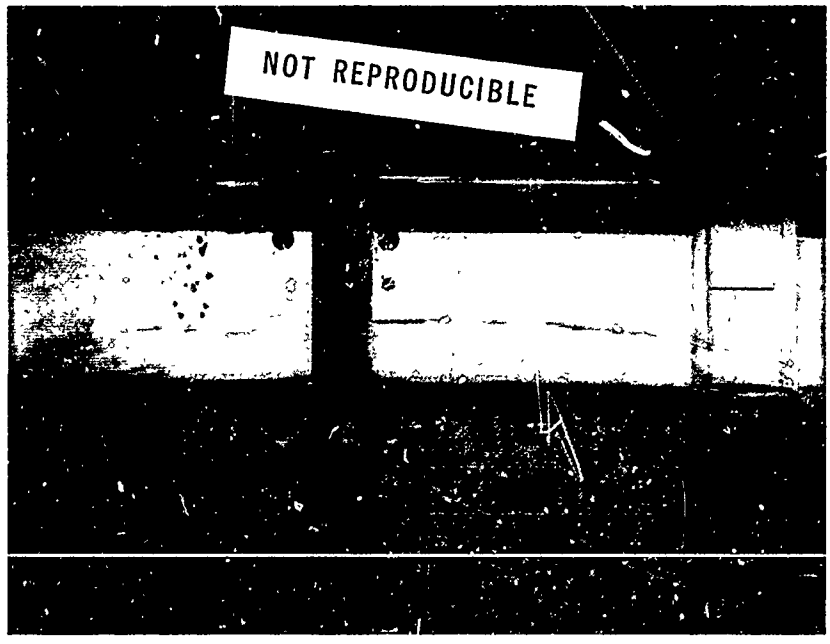

Figure 9. Spray sheets produced by strut 5B at 10 and 24 ft/sec where t/c = 0.12 and x/c = 0.65.

10 ft/sec

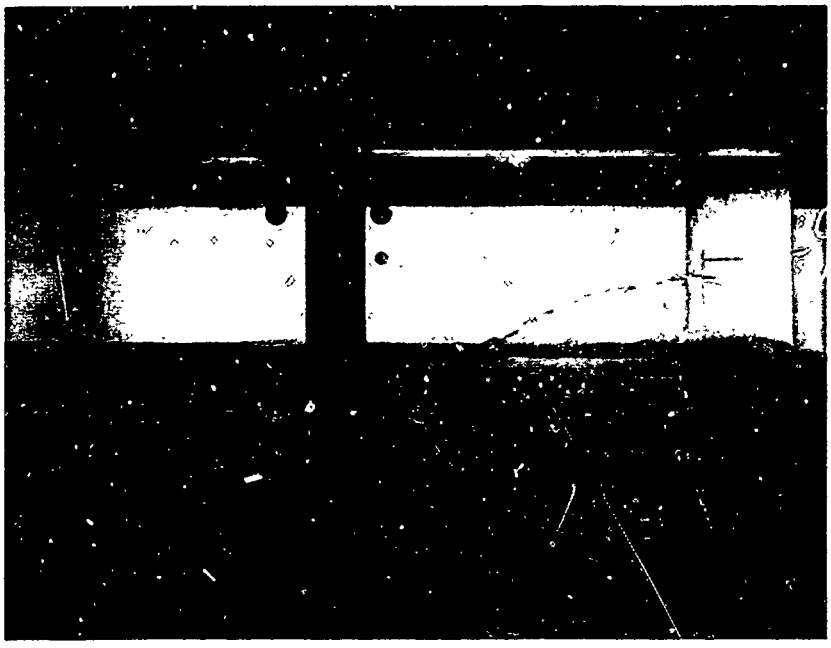

24 ft/sec

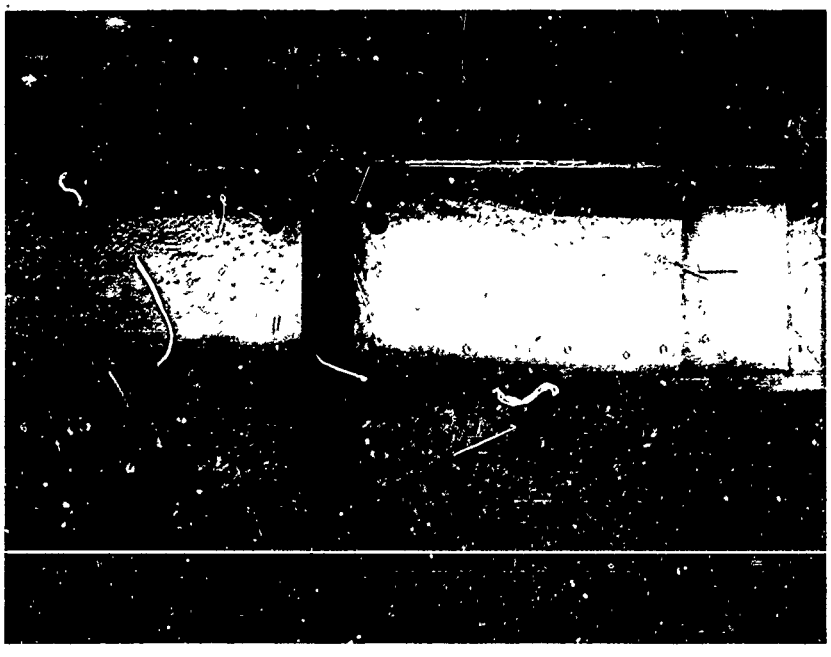

Figure 10. Spray sheets produced by strut 6 at 10 and 24 ft/sec where t/c = 0.21 and x/c = 0.50.

10 ft/sec

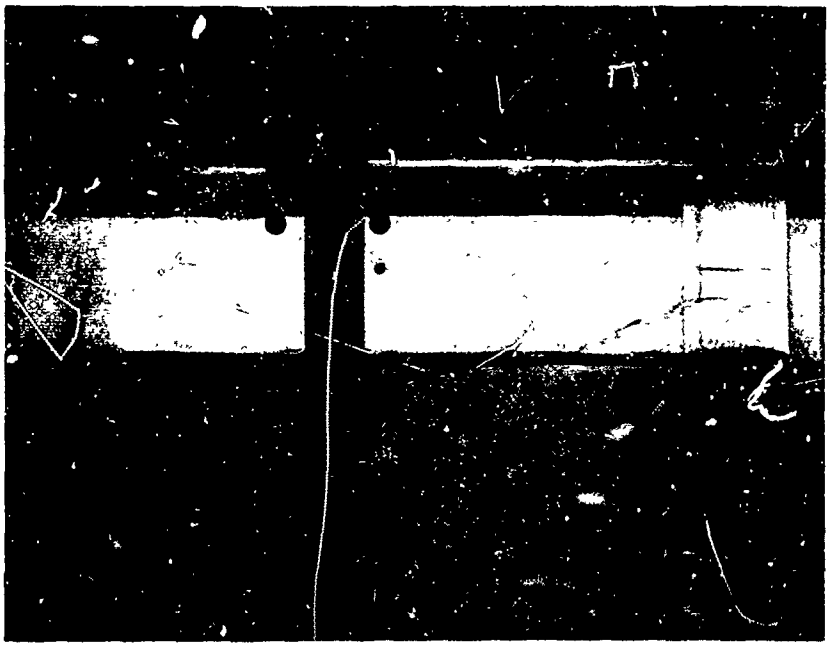

24 ft/sec

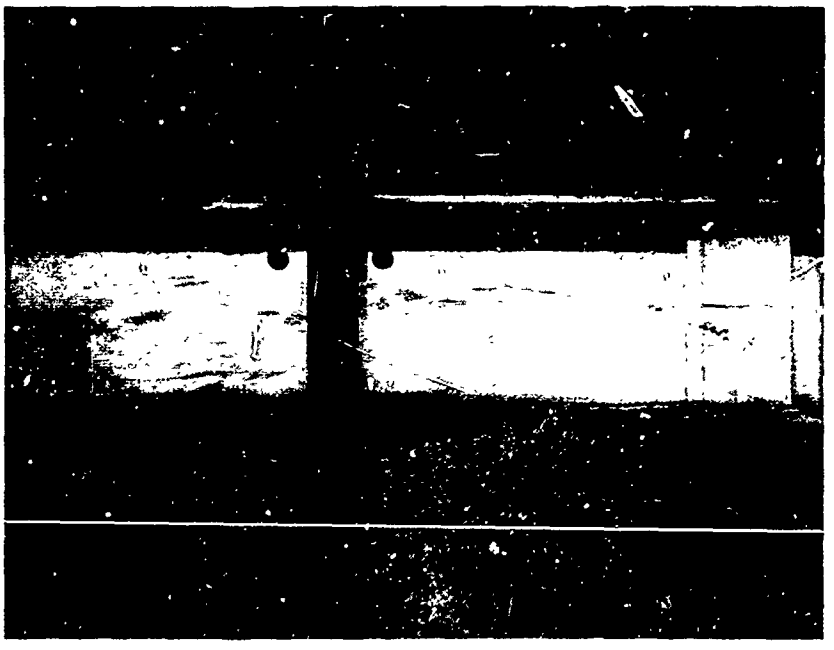

Figure 11. Spray sheets produced by strut 8A at 10 and 24 ft/sec where t/c = 0.16 (66-series airfoil).

10 ft/sec

24 ft/sec

Figure 12. Spray sheets produced by strut 9 at 10 and 24 ft/sec where t/c = 0.16 and x/c = 0.15.

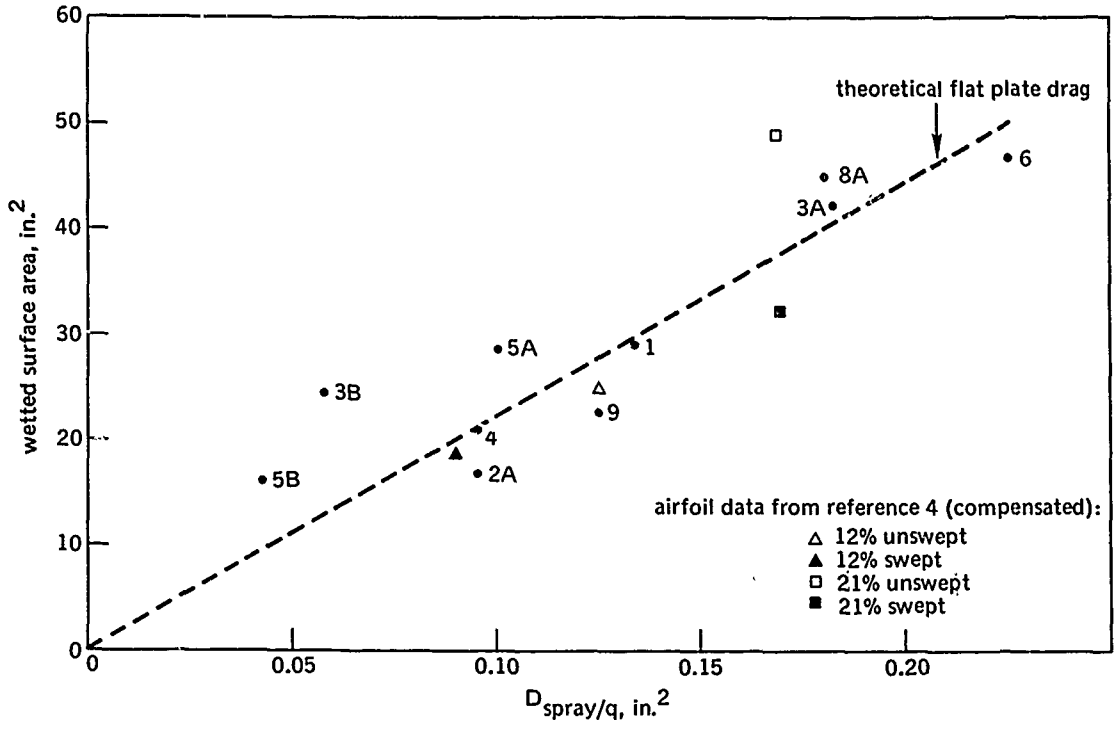

Figure 13. Variation of spray drag with surface area wetted by the spray.

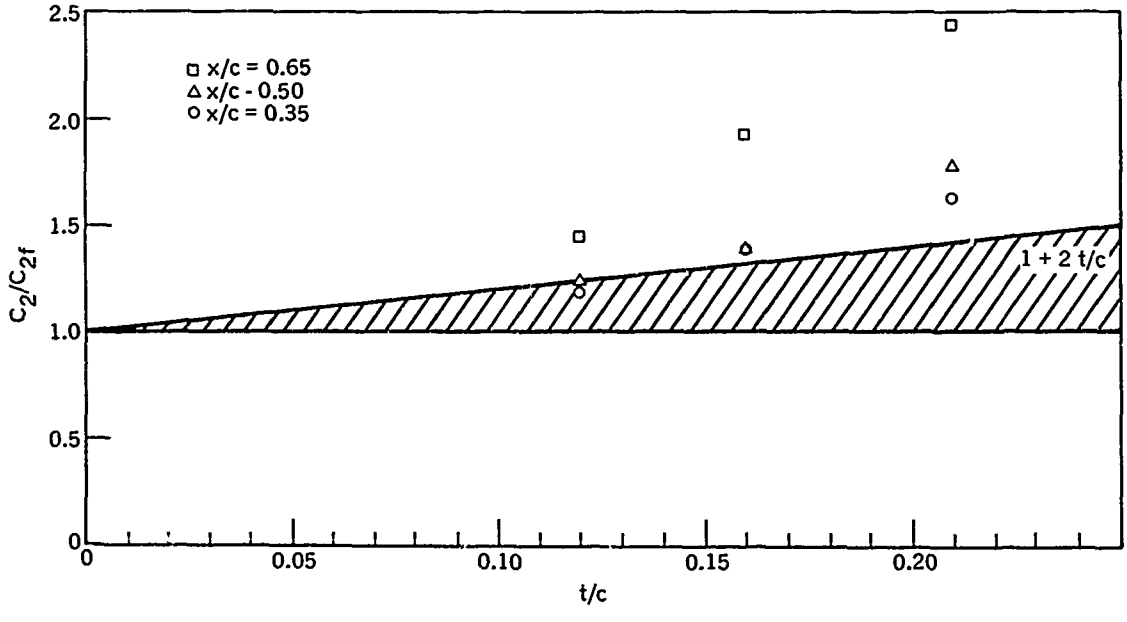

Figure 14. Ratio of section drag to flat plate skin-friction for double-arc struts.

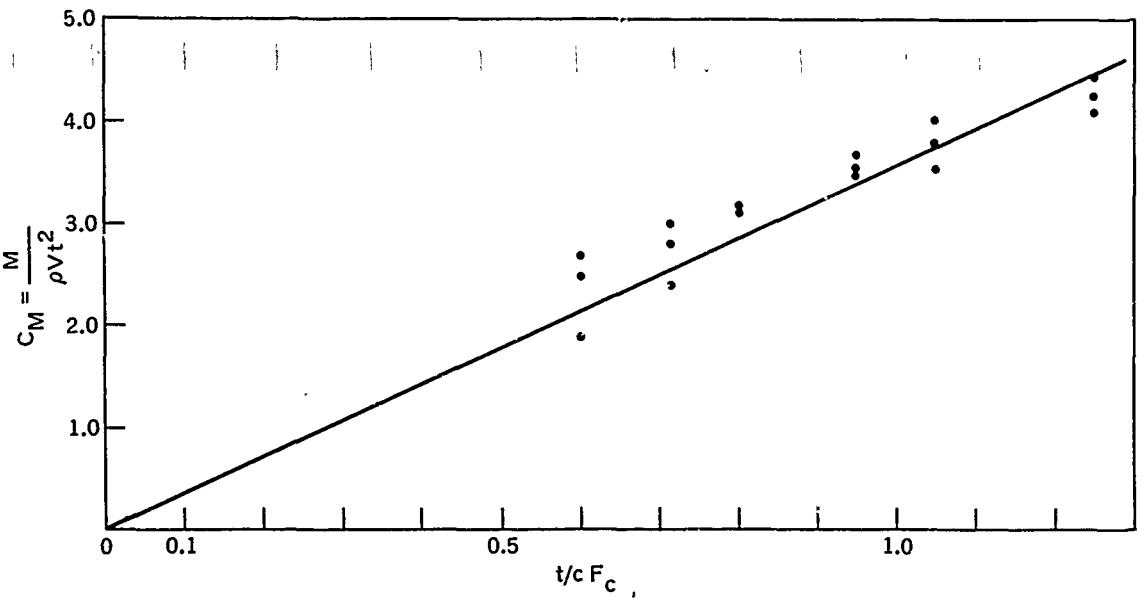

Figure 15. Variation of mass flow rate coefficient for the spray sheet with the product of the thickness ratio and Froude number.

10 ft/sec

24 ft/sec

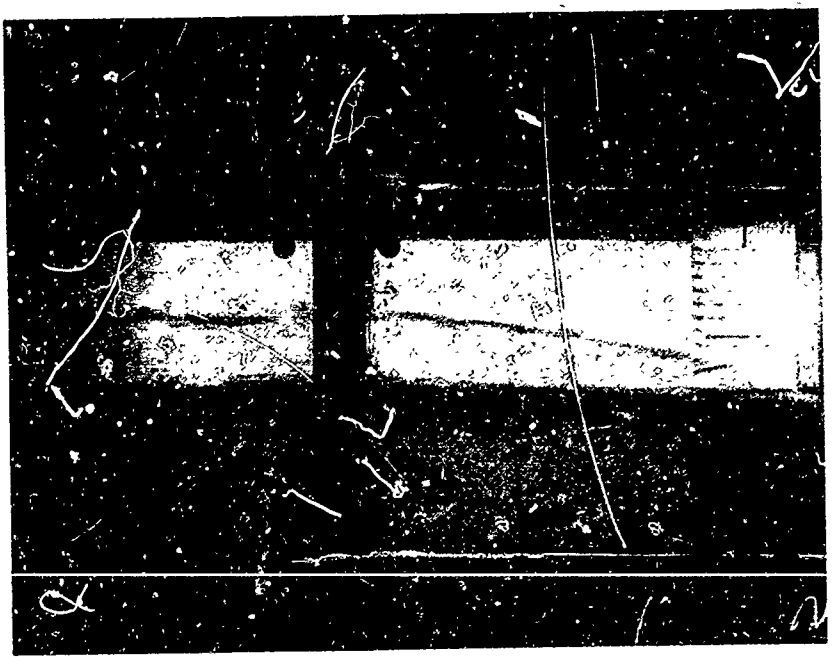

Figure 16. Effect of spray rails on spray sheets produced by strut 1 at 10 and 24 ft/sec.

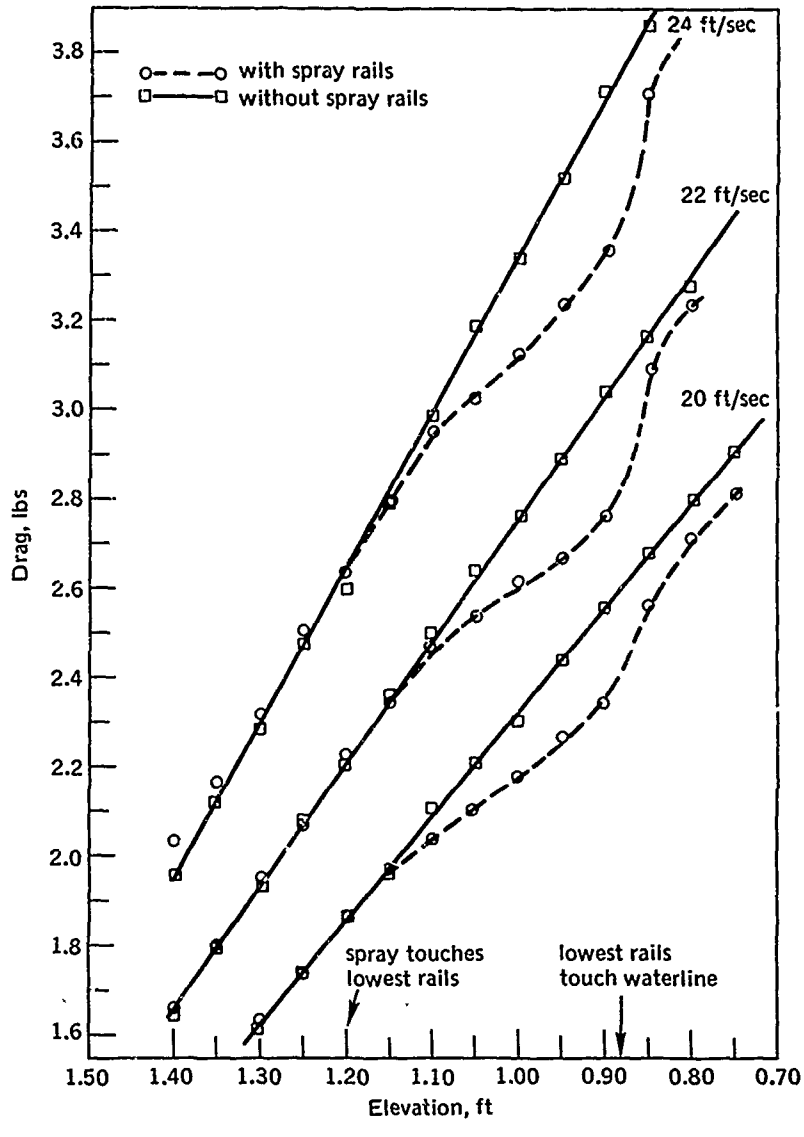

Figure 17. Effect of spray rails on drag of strut 1.

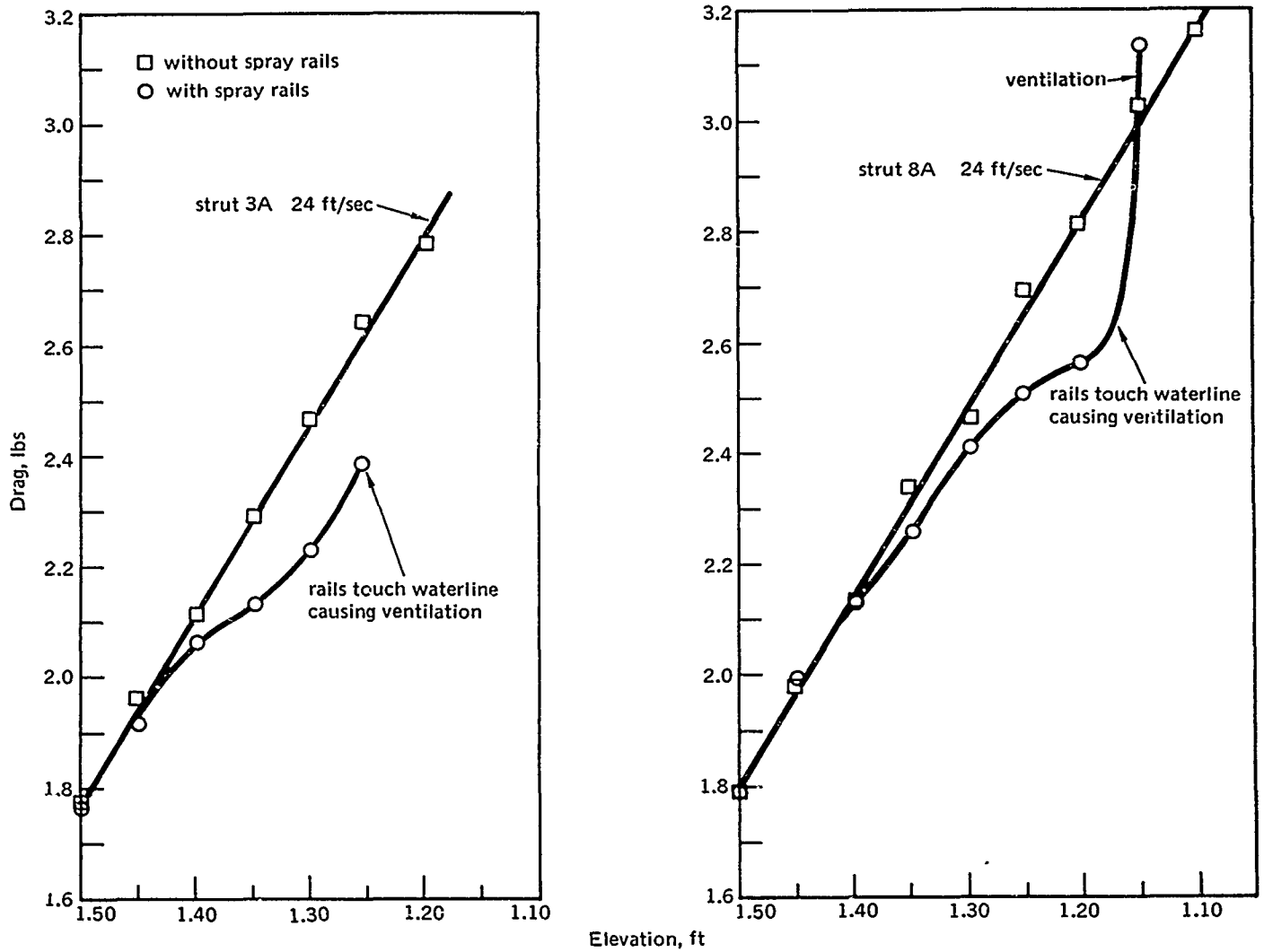

Figure 18. Effect of spray rails on drag of struts 3A and 8A.

REFERENCES

1. S. F. Hoerner. *Fluid-Dynamic Drag,* published by the author, 1965.

2. Davidson Laboratory Report 1192, *Experimental Study of Spray Drag of Some Vertical Surface-Piercing Struts,* by D. Savitsky, J. P. Breslin. December 1966.

3. Naval Undersea Research and Development Center. Technical Publication NUC TP-235, *Naval Feasibility Study of the NUC Semi-Submerged Ship Concept,* Part I: Introduction, General Characteristics, and Summary (U), by T. G. Lang. UNCLASSIFIED

4. National Advisory Committee for Aeronautics. NACA Technical Note 3092, *Hydrodynamic Drag of 12 and 21 Percent Thick Surface-Piercing Struts,* by C. W. Coffee, R. E. McKann. December 1953.

5. Stevens Institute of Technology. Stevens ETT Report 488, *Tests of Surface-Piercing Struts,* by P. Kaplan. April 1953.

6. Gibbs and Cox, Inc. Gibbs and Cox Technical Report Number 15, *Some Characteristics of Spray and Ventilation,* by S. F. Hoerner. September 1953.

7. H. Schlichting. *Boundary Layer Theory,* McGraw-Hill, 1960.

NOMENCLATURE

c	chord length
t	strut thickness
x	distance from leading edge to point of maximum thickness (forebody length)
q	dynamic pressure, $\frac{1}{2}\rho V^2$
ρ	density of water, 1.94 slugs/ft^3
V	free stream velocity
D_{total}	total drag on the strut
D_{spray}	spray drag
D_{tip}	tip drag
D_v	drag caused by the upward acceleration of the spray
X	section drag/depth of submersion
d	depth of strut tip below the waterline
P	pitching moment of strut
Z	elevation of balance above waterline
A	area of strut in the plane of the undisturbed free surface, waterplane area
C_0	spray drag coefficient, D_{spray}/qct
C_1	spray drag coefficient, D_{spray}/qA
C_2	section drag coefficient, X/qc
C_3	section drag coefficient, $X/q\sqrt{A}$
C_L	laminar component of skin-friction for two-sided plate
C_T	turbulent component of skin-friction for two-sided plate
C_{2f}	skin-friction coefficient for flat plate strut
T	thrust of spray striking plate
V'	mean velocity of spray striking plate
M	mass rate of flow of spray
C_M	mass flow rate coefficient, $M/\rho Vt^2$
F	Froude number, $V/\sqrt{gc}$
g	acceleration of gravity, 32.2 ft/sec^2
$\bar{h}$	mean maximum height of spray
ν	kinematic viscosity, 1.08×10^{-5} ft^2/sec